

# Sulfur-bearing species in molecular clouds

G. Bilalbegović<sup>1</sup>, G. Baranović<sup>2</sup>

<sup>1</sup>*Department of Physics, Faculty of Science, University of Zagreb, Bijenička 32, 10000 Zagreb, Croatia*

<sup>2</sup>*Rudjer Bošković Institute, Division of Organic Chemistry and Biochemistry, Bijenička 54, 10000 Zagreb, Croatia*

30 May 2022

## ABSTRACT

We study several molecules that could help in the solution of the missing sulfur problem in dense clouds and circumstellar regions, as well as in the clarification of the sulfur chemistry in comets. These sulfur molecules are: the trimer  $(\text{CH}_2\text{S})_3$  and the tetramer  $(\text{CH}_2\text{S})_4$  of thioformaldehyde, pentathian  $\text{S}_5\text{CH}_2$ , hexathiepan  $\text{S}_6\text{CH}_2$ , thiirane  $\text{C}_2\text{H}_4\text{S}$ , trisulfane  $\text{HSSSH}$ , and thioacetone  $(\text{CH}_3)_2\text{CS}$ . Infrared spectra of these species are calculated using density functional theory methods. The majority of calculated bands belong to the mid-infrared, with some of them occurring in the near and far-infrared region. We suggest that some of unidentified spectral features measured by *Infrared Space Observatory* in several active galactic nuclei and starburst galaxies could be caused by 1,3,5-trithiane  $((\text{CH}_2\text{S})_3)$ , 1,3,5,7-tetrathiocane  $((\text{CH}_2\text{S})_4)$ , and thiirane ( $\text{C}_2\text{H}_4\text{S}$ ). The objects whose unidentified infrared features we compare with calculated bands are: NGC 253, M82, NGC 1068, Circinus, Arp 220, 30 Doradus, Orion KL, and Sgr B2.

**Key words:** ISM: molecules – line: identification – methods: data analysis, numerical– molecular data – galaxies: ISM

## 1 INTRODUCTION

More than 180 molecules have been discovered in space (Tielens 2013). With an exception of fullerenes, the largest molecule confirmed to exist in space till now consist of thirteen atoms (Bell et al. 1997). Several sulfur-bearing molecules and ions have been observed in the interstellar medium and circumstellar shells in the Milky Way, as well as in other galaxies. The ethyl mercaptan,  $\text{CH}_3\text{CH}_2\text{SH}$ , the largest astrophysical molecule containing sulfur, was recently observed in Orion (Kolesnikova et al. 2014). Interstellar methyl mercaptan,  $\text{CH}_3\text{SH}$ , was discovered long time ago by measuring lines in the millimeter range of the spectrum toward the Sgr B2 (Linke, Frerking & Thaddeus 1979). Methyl mercaptan was also detected in other environments, for example in the organic-rich hot core G327.3-0.6 (Gibb et al. 2000), and in Orion (Kolesnikova et al. 2014). It was suggested that methyl mercaptan forms in interstellar ices and then evaporates in hot cores (Gibb et al. 2000).

Although the first interstellar sulfur-bearing molecule CS was detected a long time ago (Penzias et al. 1971), the chemistry of interstellar sulfur is still undetermined. The observed abundance of sulfur-bearing species in dense clouds is only about 0.1% of the same quantity in diffuse clouds (Tieftrunk et al. 1994; Charnley 1997). Therefore, the main sulfur species in dense regions of interstellar medium are still unknown. Molecules OCS (Palumbo, Geballe & Tielens 1997) and  $\text{SO}_2$  (Zasowski et al. 2009) were detected in in-

terstellar ices, but their abundances are not sufficient to account for the missing sulfur. Various species have been suggested as a possible reservoir of sulfur, for example polysulfanes  $\text{H}_2\text{S}_n$ , sulfur polymers  $\text{S}_n$ , solid  $\text{H}_2\text{SO}_4$ , and FeS (Druard & Wakelam 2012; Scappini et al. 2003; Keller et al. 2002). The presence of  $\text{S}^+$  and its efficient sticking to dust grains has also been proposed (Ruffle et al. 1999), as well as the existence of a substantial amount of atomic sulfur in shocked gases (Anderson et al. 2013).

Sulfur species have also been observed in comets (Festou, Uwe Keller & Weaver 2004). A cometary ice of the Hale–Bopp (C/1995 O1) had a similar IR (infrared) spectrum as interstellar ices in dense clouds (Crovisier et al. 1997; Bockelée-Morvan et al. 2000). Molecules  $\text{H}_2\text{S}$ , CS, OCS,  $\text{H}_2\text{CS}$ , and SO were observed in the comet Hale–Bopp using radio telescopes (Woodney et al. 1997; Biver et al. 1997). The low abundance of  $\text{H}_2\text{CS}$  in comparison to  $\text{H}_2\text{S}$ , as well as large daily variations in profiles and intensities of lines for  $\text{H}_2\text{S}$  and CS were found (Woodney et al. 1997). Therefore, an intensive sulfur chemistry was in progress when the comet Hale–Bopp was observed from Earth.

Models of interstellar ices containing  $\text{H}_2\text{S}$ ,  $\text{SO}_2$ , CO,  $\text{CO}_2$ ,  $\text{CH}_3\text{OH}$ ,  $\text{H}_2\text{O}$ , and/or  $\text{NH}_3$  were studied in laboratories on Earth by protons irradiation (Ferrante et al. 2008; Garozzo et al. 2010), under UV (Jiménez-Escobar & Muñoz Caro 2011; Jiménez-Escobar, Muñoz Caro & Chen 2014), and soft X-rays (Jiménez-Escobar et al. 2012). The effects of irradiation

tion and of thermal processing were explored by measuring IR and mass spectra. It was found that the amount of  $\text{H}_2\text{S}$ ,  $\text{SO}_2$ , and  $\text{CO}$  decreased and new molecules appeared. Depending on the initial ice composition, the radiation dose, and the temperature, some of detected molecules were:  $\text{OCS}$ ,  $\text{SO}_3$ ,  $\text{O}_3$ ,  $\text{H}_2\text{S}_2$ ,  $\text{HS}_2$ ,  $\text{CS}_2$ ,  $\text{H}_2\text{CO}$ ,  $\text{CH}_4$ ,  $\text{CO}_2$ ,  $\text{S}_n$ ,  $n=2-8$ . A sulfur rich residuum without IR bands also formed when the ice containing  $\text{H}_2\text{S}$  was irradiated by protons (Garozzo et al. 2010).

The thioformaldehyde molecule,  $\text{H}_2\text{CS}$ , in our galaxy was detected by measuring a higher transition  $2_{11} \leftarrow 2_{12}$  at 3139.4 MHz, in the direction of Sgr B2 (Sinclair et al. 1973).  $\text{H}_2\text{CS}$  was observed in cold and hot cores, outflows of stars, and in the interstellar medium (Maeda et al. 2008). Thioformaldehyde was also observed in other galaxies (Heikkila, Johansson & Olofsson 1999; Martin et al. 2005). The  $\text{H}_2\text{CS}$  molecule is unstable under laboratory conditions on Earth (Peach, Weissflog & Pelz 1975). It is prone to polymerization and, as possible products, various cyclic molecules might occur. Among simplest ones are  $(\text{CH}_2\text{S})_3$  (1,3,5-trithiane) and  $(\text{CH}_2\text{S})_4$  (1,3,5,7-tetrathiocane). Properties of higher polymeric thioformaldehydes,  $(\text{CH}_2\text{S})_n$ , have also been studied on Earth (Credali & Russo 1967; Peach, Weissflog & Pelz 1975). The cyclic structures,  $(\text{CH}_2\text{S})_n$ , are stable. Thus, they appear as a possible reservoir of sulfur in space. In laboratories  $(\text{CH}_2\text{S})_3$  forms when formaldehyde and hydrogen sulfide react. Various routes and catalysts for this reaction have been found. One way to form  $(\text{CH}_2\text{S})_3$  is the reaction between  $\text{H}_2\text{CO}$  and  $\text{H}_2\text{S}$  under irradiation (Credali & Russo 1967). Both  $\text{H}_2\text{CO}$  and  $\text{H}_2\text{S}$  have been discovered in our and other galaxies (Snyder et al. 1969; Gardner & Whiteoak 1974; Thaddeus et al. 1972; Heikkila, Johansson & Olofsson 1999). It was proposed that formaldehyde forms in interstellar ices by hydrogenation of  $\text{CO}$  (Tielens & Whittet 1997; Watanabe & Kouchi 2002). The observed abundances of  $\text{H}_2\text{S}$  are such that it has been assumed that this molecule also forms in interstellar ices on dust grains (Charnley 1997; Buckle & Fuller 2003). We expect that, as in chemical laboratories on Earth, formaldehyde and hydrogen sulfide react in space under irradiation (such as UV, X, or cosmic rays), and that  $(\text{CH}_2\text{S})_3$  and higher polymeric thioformaldehydes are present. Formaldehyde and hydrogen sulfide (Biver et al. 1997), as well as thioformaldehyde (Woodney et al. 1997), were also detected in the Hale-Bopp. In addition, several other sulfur-bearing species and changes of intensities for  $\text{H}_2\text{S}$  during observations were detected in this comet. It is possible to suggest that formaldehyde and hydrogen sulfide react in the Hale-Bopp (and perhaps in some other comets) and form cyclic thioformaldehydes.

Cyclic molecules pentathian ( $\text{S}_5\text{CH}_2$ ) and hexathiepan ( $\text{S}_6\text{CH}_2$ ) were detected in laboratory astrophysics experiments on interstellar ices after the UV irradiation at  $T=12$  K, which was followed by heating to room temperature (Muñoz Caro 2002). Mass spectra were measured and, among pentathian, hexathiepan and some known molecules, several unidentified species were found. This opens a possibility that  $(\text{CH}_2\text{S})_3$ ,  $(\text{CH}_2\text{S})_4$  and other sulfur-bearing species were also present, or could be formed under suitable conditions. Disulfane,  $\text{H}_2\text{S}_2$ , was also detected in laboratory experiments on interstellar ices (Ferrante et al. 2008; Garozzo et al. 2010; Jiménez-Escobar & Muñoz Caro

2011; Jiménez-Escobar et al. 2012; Jiménez-Escobar, Muñoz Caro & Chen 2014). The presence of polysulfanes,  $\text{H}_2\text{S}_n$ , was suggested (Druard & Wakelam 2012). The results of calculations on chemical networks predicted that  $\text{H}_2\text{S}_3$  is more abundant than  $\text{H}_2\text{S}_2$  in less dense clouds at  $T=20$  K (Druard & Wakelam 2012). Therefore,  $\text{H}_2\text{S}_3$  is an important molecule for further studies of sulfur species in molecular clouds. We investigate the most stable conformation *trans*-HSSSH (Liedtke et al. 1993). Thioacetone,  $(\text{CH}_3)_2\text{CS}$ , in the form we study, consists of the two methyl groups and the sulfur atom doubly bonded to carbon that could give rise to specific IR spectral features. Thioacetone could exist as the thioketo and thienol tautomers, but thioenol transforms to the thioketo form (Lipscomb & Sharkey 1970). We study the thioketo tautomer that is prone to polymerization, and therefore unstable. However, its lifetime is several minutes (Kroto et al. 1974). Thiirane ( $\text{C}_2\text{H}_4\text{S}$ , ethylene sulfide) is the smallest cyclic molecule containing sulfur. Its oxygen analogue oxirane ( $\text{C}_2\text{H}_4\text{O}$ ) is already confirmed as an astrophysical molecule (Dickens et al. 1997; Puzzarini et al. 2014).

Most sulfur-bearing and other astrophysical molecules have been detected by radio telescopes involving rotational spectra. For some of molecules studied here by calculating their infrared spectra, rotational spectra and constants are available:  $(\text{CH}_2\text{S})_3$  (Antolinez et al. 2002; Cervellati, Corbelli & Lister 1984; Dorofeeva & Gurvich 1995), *trans*-HSSSH (Liedtke et al. 1993, 1997),  $(\text{CH}_3)_2\text{CS}$  (Kroto et al. 1974),  $\text{C}_2\text{H}_4\text{S}$  (Hirao, Okabayashi & Tanimoto 2001; Kirchner et al. 1997; Hirose, Okiye & Maeda 1976).

In this work, to shed light on the missing reservoirs of sulfur in dense interstellar clouds, we study several sulfur-bearing species. This study is also important for understanding of the sulfur chemistry in comets. IR spectra of sulfur molecules are calculated using density functional theory methods (Becke 2014). In Sec. 2 we describe computational methods. In Sec. 3.1 we present the calculated properties of molecules and their IR spectra. We compare calculated bands with observed spectra of astrophysical objects and find good agreement between some calculated bands and unidentified features observed by *Infrared Space Observatory (ISO)* in several starburst and active galaxies (ISO 2002; Sturm et al. 2000; Lutz et al. 2000; Fischer et al. 1999). Therefore, in Sec. 3.2 we present the list of already detected sulfur-bearing species in molecular gases of these galaxies and briefly describe conditions for their formation. In Sec. 3.3 we list detected sulfur-bearing species in environments of our galaxy: Orion KL and Sgr B2. The conclusions are summarized in Sec. 4.

## 2 COMPUTATIONAL METHODS

We use density functional theory methods within the Gaussian code (Frisch et al. 2013) to study several sulfur-bearing molecules. The hybrid B3LYP functional (Becke 1993; Stephens et al. 1994) and the augmented correlation consistent aug-cc-pVTZ basis set (Woon & Dunning 1993) are applied. It was found that this basis set and the B3LYP functional produced accurate IR intensities

(Zvereva, Shagidullin & Katsyuba 2011). Using these methods we compute harmonic vibrational frequencies.

The Gaussian code and B3LYP functional have been successfully applied for studies of IR spectra of interstellar molecules and nanoparticles (Bauschlicher et al. 2010; Boersma et al. 2014; Ricca et al. 2012; Goumans & Bromley 2011). Scale factors are used in this type of calculations (Bauschlicher et al. 2010) to minimize errors due to anharmonic effects, basis set incompleteness and unknown exchange-correlation effects in density functional theory approximations. The other, more rigorous, way is to do vibrational calculations with anharmonic correction to frequencies and intensities. We tested a new implementation of full anharmonic IR intensities at the second-order of perturbation theory level (Bloino & Barone 2012; Barone et al. 2010). However, we found that the present implementation of this method (in the Gaussian 09 code) is not suitable for the  $C_{3v}$  symmetry of  $(\text{H}_2\text{CS})_3$ .

In this work nine molecules ( $\text{CS}_2$  (Shimanouchi 1972),  $\text{C}_2\text{H}_4\text{S}$  (Allen et al. 1986),  $\text{C}_2\text{H}_4\text{O}$  (Puzzarini et al. 2014),  $\text{HS}_2\text{H}$  (Jacox 1994),  $\text{H}_2\text{CS}$  (Jacox 1994),  $\text{CH}_3\text{SH}$  (Sverdlov, Kovner & Krainov 1974),  $\text{CH}_3\text{SCH}_3$  (Sverdlov, Kovner & Krainov 1974),  $\text{SO}_2$  (Person & Zerbi 1982), and  $\text{H}_2\text{S}$  (Shimanouchi 1972)) were used to obtain the value of 0.9687 for the scaling factor. The mean average error, the mean absolute error, and the root mean square error were 7.7, 18.9 and 23.1  $\text{cm}^{-1}$ , respectively. The calculated intensities for the nine molecules were in good agreement with experiment what was actually expected from the chosen level of theory (B3LYP/aug-cc-pVTZ). The calculated frequencies of  $(\text{CH}_2\text{S})_3$ ,  $(\text{CH}_2\text{S})_4$ ,  $\text{S}_5\text{CH}_2$ ,  $\text{S}_6\text{CH}_2$ ,  $\text{HSSSH}$ ,  $(\text{CH}_3)_2\text{CS}$ , and  $\text{C}_2\text{H}_4\text{S}$  were subsequently scaled with 0.9687 and, together with calculated intensities, used for astrophysical predictive purposes. For IR spectra presented in this work we used Lorentzian band profiles with FWHM of 15  $\text{cm}^{-1}$ .

### 3 RESULTS AND DISCUSSION

#### 3.1 Infrared Spectra

Figs. 1-3 show optimized geometries of molecules we study. Both  $(\text{CH}_2\text{S})_3$  and  $(\text{CH}_2\text{S})_4$  are chair-shaped cyclic structures (Fig. 1), where rings are composed of, respectively, six and eight alternating C and S atoms. In contrast, in the rings of  $\text{S}_5\text{CH}_2$  and  $\text{S}_6\text{CH}_2$  (Fig. 2) only one carbon atom exists, whereas two C atoms appear in the cyclic structure of  $\text{C}_2\text{H}_4\text{S}$  (Fig. 3 (c)). Zig-zag (or helix) structures of either S, or C atoms exist for, respectively,  $\text{HSSSH}$  (Fig. 3 (a)) and  $\text{C}_3\text{H}_6\text{S}$  (Fig. 3 (b)). The coordinates of optimized structures for all molecules are available as the online-only supporting information.

We have calculated that  $(\text{CH}_2\text{S})_3$  has a large dipole moment of 2.1787 Debye. In contrast the dipole moment of  $(\text{CH}_2\text{S})_4$  is zero. It is known that molecules with a zero dipole moment are radio inactive. Therefore,  $(\text{CH}_2\text{S})_4$  could only be detected in the IR spectral region and for radio telescopes this molecule would behave as the hidden part of a possible reservoir of sulfur. Dipole moments of 1.9784, 1.7086, 1.9669, 0.5085, 2.9493 Debye are calculated for  $\text{S}_5\text{CH}_2$ ,  $\text{S}_6\text{CH}_2$ ,  $\text{C}_2\text{H}_4\text{S}$ ,  $\text{HSSSH}$ ,  $(\text{CH}_3)_2\text{CS}$ , respectively.

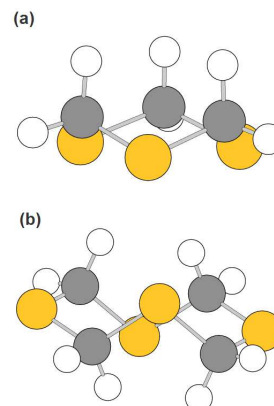


**Figure 1.** The optimized structures: (a)  $(\text{CH}_2\text{S})_3$  (thioformaldehyde trimer, 1,3,5-trithiane), (b)  $(\text{CH}_2\text{S})_4$  (thioformaldehyde tetramer, 1,3,5,7-tetrathiocane). Small white balls represent hydrogen atoms, light gray (yellow in the color figure) are for sulfur atoms, and dark gray for carbon atoms.

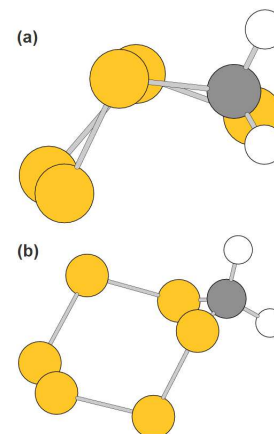


**Figure 2.** The optimized structures: (a)  $\text{S}_5\text{CH}_2$  (pentathian), (b)  $\text{S}_6\text{CH}_2$  (hexathiepan). Details as in Fig. 1.

Our results for IR spectra are shown in Figs. 4-6, whereas the bands and their intensities are presented in Tables 1-7. Relative intensities of calculated bands shown in these Tables are determined as percentage of the strongest band. Relative intensities of measured bands are known only qualitatively (v-very, s-strong, m-mean, w-weak, e-extremely), and were after (Klaboe 1969; Ellestad et al. 1972; Wiesier et al. 1969) assigned a quantitative measure by dividing the interval from 0 to 1 into six equal parts.

In  $(\text{CH}_2\text{S})_3$  the strongest calculated band at 14.46  $\mu\text{m}$  is dominantly due to the C-S stretching (Table 1). The same is valid for the pair of the  $(\text{CH}_2\text{S})_4$  calculated rather strong bands at 12.66 and 13.96  $\mu\text{m}$  (Table 2). The strongest calculated band of  $(\text{CH}_2\text{S})_4$  is at 14.43  $\mu\text{m}$ . We are not aware of any existing measured IR vibrational data concerning pentathian and hexathiepan. The vibrational normal modes involving sulfur atoms are generally weak. This is particularly well seen in pentathian and hexathiepan where the strongest bands, respectively at 23.93 and 22.31  $\mu\text{m}$ , are only 10.13 and 6.41  $\text{km mol}^{-1}$  strong (Tables 3 and 4).

In the case of  $\text{HSSSH}$ , the strong band calculated at

**Table 1.** Calculated (scaled by 0.9687) and measured <sup>a</sup>(Klaboe 1969; Ellestad et al. 1972) vibrational fundamentals for 1,3,5 trithiane, (CH<sub>2</sub>S)<sub>3</sub>. After IR measurements in vapour <sup>a</sup>(Klaboe 1969; Ellestad et al. 1972) we labeled relative intensities of experimental bands with: s (strong), m (medium), w (weak) and v (very). Three IR inactive A<sub>2</sub> modes (from 8 to 10) are omitted.

| Calculated |                |                                   |                      |                                 | Measured <sup>a</sup> |                                   |                      |           |
|------------|----------------|-----------------------------------|----------------------|---------------------------------|-----------------------|-----------------------------------|----------------------|-----------|
| Mode       | Symm.          | $\tilde{\nu}$ (cm <sup>-1</sup> ) | $\lambda$ ( $\mu$ m) | IR int. (km mol <sup>-1</sup> ) | Rel. int.             | $\tilde{\nu}$ (cm <sup>-1</sup> ) | $\lambda$ ( $\mu$ m) | Rel. int. |
| 1          | A <sub>1</sub> | 3027.2                            | 3.30                 | 1.08                            | 3                     | -                                 | -                    | -         |
| 2          |                | 2947.9                            | 3.39                 | 31.03                           | 99                    | 2900                              | 3.45                 | vs        |
| 3          |                | 1392.5                            | 7.18                 | 8.95                            | 28                    | 1378                              | 7.26                 | s         |
| 4          |                | 888.4                             | 11.26                | 9.77                            | 31                    | 898                               | 11.14                | s         |
| 5          |                | 622.4                             | 16.07                | 2.19                            | 7                     | 655                               | 15.27                | s         |
| 6          |                | 381.2                             | 26.23                | 0.02                            | 0                     | 398                               | 25.13                | vw        |
| 7          |                | 274.8                             | 36.39                | 1.56                            | 5                     | 308                               | 32.47                | m         |
| 11         | E              | 3028.7                            | 3.30                 | 0.02                            | 0                     | 2980                              | 3.36                 | s         |
| 12         |                | 2953.4                            | 3.39                 | 3.95                            | 13                    | -                                 | -                    | -         |
| 13         |                | 1379.4                            | 7.25                 | 2.85                            | 9                     | 1394                              | 7.17                 | vs        |
| 14         |                | 1204.5                            | 8.30                 | 13.31                           | 42                    | 1211                              | 8.26                 | vs        |
| 15         |                | 1151.7                            | 8.68                 | 13.84                           | 44                    | 1162                              | 8.61                 | vs        |
| 16         |                | 769.6                             | 13.00                | 0.04                            | 0                     | 802                               | 12.47                | w         |
| 17         |                | 691.3                             | 14.46                | 31.48                           | 100                   | 728                               | 13.74                | vs        |
| 18         |                | 629.2                             | 15.89                | 3.01                            | 10                    | 655                               | 15.27                | s         |
| 19         |                | 268.3                             | 37.27                | 1.60                            | 5                     | 280                               | 35.71                | m         |
| 20         |                | 169.4                             | 59.03                | 0.00                            | 0                     | -                                 | -                    | -         |

**Table 2.** Calculated (scaled by 0.9687) and measured <sup>a</sup>(Nash, Kenneth Musker & Lam 1988) vibrational A<sub>u</sub> fundamentals for 1,3,5,7-tetrathiocane, (CH<sub>2</sub>S)<sub>4</sub>. Twenty one IR inactive A<sub>g</sub> modes are omitted. Details for relative intensities of measured bands as in Table 1.

| Calculated |                |                                   |                      |                                 | Measured <sup>a</sup> |                                   |                      |           |
|------------|----------------|-----------------------------------|----------------------|---------------------------------|-----------------------|-----------------------------------|----------------------|-----------|
| Mode       | Symm.          | $\tilde{\nu}$ (cm <sup>-1</sup> ) | $\lambda$ ( $\mu$ m) | IR int. (km mol <sup>-1</sup> ) | Rel. int.             | $\tilde{\nu}$ (cm <sup>-1</sup> ) | $\lambda$ ( $\mu$ m) | Rel. int. |
| 1          | A <sub>u</sub> | 3035.9                            | 3.29                 | 3.92                            | 6                     | -                                 | -                    | -         |
| 2          |                | 3031.5                            | 3.30                 | 2.72                            | 4                     | -                                 | -                    | -         |
| 3          |                | 2980.7                            | 3.35                 | 7.17                            | 11                    | -                                 | -                    | -         |
| 4          |                | 2978.1                            | 3.36                 | 14.39                           | 23                    | -                                 | -                    | -         |
| 5          |                | 1400.1                            | 7.14                 | 26.34                           | 42                    | 1397                              | 7.16                 | s         |
| 6          |                | 1376.0                            | 7.27                 | 5.51                            | 9                     | 1360                              | 7.35                 | m         |
| 7          |                | 1210.7                            | 8.26                 | 49.84                           | 79                    | 1212                              | 8.25                 | m         |
| 8          |                | 1203.7                            | 8.31                 | 29.81                           | 47                    | 1207                              | 8.29                 | s         |
| 9          |                | 1136.6                            | 8.80                 | 6.93                            | 11                    | 1137                              | 8.80                 | vw        |
| 10         |                | 1122.2                            | 8.91                 | 6.89                            | 11                    | -                                 | -                    | -         |
| 11         |                | 797.4                             | 12.54                | 2.22                            | 4                     | 804                               | 12.44                | m         |
| 12         |                | 789.7                             | 12.66                | 19.86                           | 31                    | 750                               | 13.33                | vs        |
| 13         |                | 716.6                             | 13.96                | 28.23                           | 45                    | 732                               | 13.66                | vs        |
| 14         |                | 692.8                             | 14.43                | 63.27                           | 100                   | 715                               | 13.99                | m         |
| 15         |                | 610.6                             | 16.38                | 8.40                            | 13                    | 631                               | 15.85                | w         |
| 16         |                | 599.4                             | 16.69                | 7.67                            | 12                    | 614                               | 16.29                | vw        |
| 17         |                | 365.3                             | 27.37                | 0.61                            | 1                     | -                                 | -                    | -         |
| 18         |                | 278.5                             | 35.91                | 7.56                            | 12                    | -                                 | -                    | -         |
| 19         |                | 195.2                             | 51.23                | 1.65                            | 3                     | -                                 | -                    | -         |
| 20         |                | 128.1                             | 78.07                | 3.55                            | 6                     | -                                 | -                    | -         |
| 21         |                | 31.1                              | 321.71               | 4.21                            | 7                     | -                                 | -                    | -         |

22.82  $\mu$ m is the antisymmetric S-S stretching (Table 5). Vibrational spectra of H<sub>2</sub>S<sub>3</sub> were first measured in CCl<sub>4</sub> and CS<sub>2</sub> solutions, but the *cis* conformer was assigned as a carrier (Wiesier et al. 1969). More recently, the IR spectrum of H<sub>2</sub>S<sub>3</sub> was measured in the gas phase in the range from 400 to 4000 cm<sup>-1</sup>, but unfortunately with a low resolution, and only frequencies measured at 2548, 865, and 480 cm<sup>-1</sup> were reported (Liedtke et al. 1993). However, both measure-

ments (Wiesier et al. 1969; Liedtke et al. 1993) and our results show that IR frequencies of *trans* and *cis* conformers are similar. In Table 5 we compare our results with detailed measurements (Wiesier et al. 1969). Liedtke and coworkers also reported the calculated IR frequencies done using the Moller-Plesset perturbation operator (MP2) and the MC-311G(d,p) basis set. Their frequencies are unscaled

**Table 3.** Calculated (scaled by 0.9687) vibrational fundamentals bands for pentathian, S<sub>5</sub>CH<sub>2</sub>.

| Mode | $\tilde{\nu}$ (cm <sup>-1</sup> ) | $\lambda$ ( $\mu$ m) | IR int. (km mol <sup>-1</sup> ) | Rel. int. |
|------|-----------------------------------|----------------------|---------------------------------|-----------|
| 1    | 3024.4                            | 3.31                 | 0.39                            | 4         |
| 2    | 2960.1                            | 3.38                 | 8.75                            | 86        |
| 3    | 1390.7                            | 7.19                 | 1.43                            | 14        |
| 4    | 1175.6                            | 8.51                 | 2.06                            | 20        |
| 5    | 1084.8                            | 9.22                 | 0.12                            | 1         |
| 6    | 813.0                             | 12.30                | 2.58                            | 25        |
| 7    | 670.2                             | 14.92                | 1.18                            | 12        |
| 8    | 599.4                             | 16.68                | 1.57                            | 16        |
| 9    | 486.0                             | 20.58                | 2.57                            | 25        |
| 10   | 474.4                             | 21.08                | 0.43                            | 4         |
| 11   | 417.9                             | 23.93                | 10.13                           | 100       |
| 12   | 357.6                             | 27.96                | 0.26                            | 3         |
| 13   | 342.5                             | 29.19                | 2.07                            | 20        |
| 14   | 241.5                             | 41.41                | 0.08                            | 1         |
| 15   | 222.0                             | 45.05                | 0.09                            | 1         |
| 16   | 189.9                             | 52.65                | 0.58                            | 6         |
| 17   | 173.2                             | 57.72                | 2.35                            | 23        |
| 18   | 35.2                              | 284.29               | 0.60                            | 6         |

**Table 4.** Calculated (scaled by 0.9687) vibrational fundamentals bands for hexathiepan, S<sub>6</sub>CH<sub>2</sub>.

| Mode | $\tilde{\nu}$ (cm <sup>-1</sup> ) | $\lambda$ ( $\mu$ m) | IR int. (km mol <sup>-1</sup> ) | Rel. int. |
|------|-----------------------------------|----------------------|---------------------------------|-----------|
| 1    | 3006.8                            | 3.33                 | 2.29                            | 36        |
| 2    | 2951.7                            | 3.39                 | 2.37                            | 37        |
| 3    | 1386.2                            | 7.21                 | 1.38                            | 22        |
| 4    | 1175.2                            | 8.51                 | 4.78                            | 75        |
| 5    | 1094.9                            | 9.13                 | 0.02                            | 0         |
| 6    | 790.8                             | 12.65                | 3.21                            | 50        |
| 7    | 688.0                             | 14.53                | 2.87                            | 45        |
| 8    | 591.3                             | 16.91                | 0.01                            | 0         |
| 9    | 460.5                             | 21.71                | 1.46                            | 23        |
| 10   | 456.6                             | 21.90                | 1.44                            | 23        |
| 11   | 448.3                             | 22.31                | 6.41                            | 100       |
| 12   | 403.0                             | 24.81                | 0.52                            | 8         |
| 13   | 373.0                             | 26.81                | 1.08                            | 17        |
| 14   | 347.3                             | 28.79                | 0.00                            | 0         |
| 15   | 270.6                             | 36.96                | 0.47                            | 7         |
| 16   | 228.7                             | 43.73                | 1.07                            | 17        |
| 17   | 193.0                             | 51.81                | 4.17                            | 65        |
| 18   | 174.8                             | 57.21                | 0.07                            | 1         |
| 19   | 161.3                             | 62.01                | 0.53                            | 8         |
| 20   | 111.0                             | 90.07                | 0.23                            | 4         |
| 21   | 43.5                              | 229.67               | 2.03                            | 32        |

and bands start at much higher (for 243 cm<sup>-1</sup>) values than experimental and these we calculated.

The only band of thioacetone worth of searching for in space should be a very strong C=S stretching band calculated at 8.01  $\mu$ m (Table 6). Thiirane can be detected by measuring its two strongest bands calculated at 16.68 and 9.57  $\mu$ m (Table 7). The former can be described as a symmetric C-S stretching, while the latter as a CH<sub>2</sub> wagging. First fourteen modes in the IR spectra of thiirane were measured and assigned by (Allen et al. 1986). Recently, far-IR modes at 760–400 and 170–10 cm<sup>-1</sup> were studied using the synchrotron light source (Bane et al. 2012). Two modes  $\nu_5 = 628.1$  and  $\nu_{15} = 669.7$  cm<sup>-1</sup> were measured, as well as subsequently calculated at the B3LYP/cc-pVTZ level, and then fitted.

For all molecules we study some other rather strong bands exist, but they are typical for the C-H bonds. Thus, these bands are less suitable for a search of the sulfur-bearing species in space.

In Table 8 we compare calculated bands of (CH<sub>2</sub>S)<sub>3</sub>, (CH<sub>2</sub>S)<sub>4</sub>, and C<sub>2</sub>H<sub>4</sub>S with unidentified features observed by *ISO* in, either galaxies known for their starburst activity, or galaxies with active galactic nuclei: M82, NGC 253, the 30 Doradus star-forming region in the Large Magellanic Cloud, NGC 1068, Circinus, Arp 220 (ISO 2002; Sturm et al. 2000; Lutz et al. 2000; Fischer et al. 1999). We find that in the interval around unidentified bands, determined by the scaling factor used within density functional theory method, belong ten calculated bands of (CH<sub>2</sub>S)<sub>3</sub>, eleven of (CH<sub>2</sub>S)<sub>4</sub>, and five of C<sub>2</sub>H<sub>4</sub>S. For all three species

**Table 5.** Calculated (scaled by 0.9687) and measured <sup>a</sup>(Wiesier et al. 1969) fundamental vibrational bands for HSSSH. Relative intensities of experimental bands are labeled with: sh (shoulder), m (medium), and strong (s).

| Calculated |       |                                   |                      |                                 | Measured <sup>a</sup> |                                   |                      |           |
|------------|-------|-----------------------------------|----------------------|---------------------------------|-----------------------|-----------------------------------|----------------------|-----------|
| Mode       | Symm. | $\tilde{\nu}$ (cm <sup>-1</sup> ) | $\lambda$ ( $\mu$ m) | IR int. (km mol <sup>-1</sup> ) | Rel. int.             | $\tilde{\nu}$ (cm <sup>-1</sup> ) | $\lambda$ ( $\mu$ m) | Rel. int. |
| 1          | A     | 2548.6                            | 3.92                 | 0.48                            | 2                     | 2540                              | 3.94                 | sh        |
| 3          |       | 841.9                             | 11.88                | 0.04                            | 0                     | 868                               | 11.52                | sh        |
| 5          |       | 458.8                             | 21.79                | 0.10                            | 0                     | 487                               | 20.53                | sh        |
| 8          |       | 303.4                             | 32.96                | 17.20                           | 58                    | -                                 | -                    | -         |
| 9          |       | 193.7                             | 51.63                | 0.00                            | 0                     | -                                 | -                    | -         |
| 2          | B     | 2547.1                            | 3.93                 | 0.90                            | 3                     | 2532                              | 3.95                 | m         |
| 4          |       | 829.2                             | 12.06                | 8.54                            | 29                    | 856                               | 11.68                | m         |
| 6          |       | 438.2                             | 22.82                | 29.67                           | 100                   | 477                               | 20.96                | s         |
| 7          |       | 322.2                             | 31.04                | 11.77                           | 40                    | -                                 | -                    | -         |

**Table 6.** Calculated (scaled by 0.9687) and measured vibrational fundamental bands for thioacetone, (CH<sub>3</sub>)<sub>2</sub>CS. Measured bands are from <sup>a</sup>(Lipscomb & Sharkey 1970) and <sup>b</sup>(NIST 2014) in vapour, as well as from <sup>c</sup>(Garrigou-Lagrange and C. G. Andrieu and Y. Mollier 1974) in liquid. Relative intensities of experimental bands are labeled with: m (medium), s (strong), and vs (very strong). Raman measurements in liquid are labeled by r.

| Calculated |                |                                   |                      |                                 | Measured <sup>a,b</sup> |                                   |                      | Measured <sup>c</sup>             |                      |           |
|------------|----------------|-----------------------------------|----------------------|---------------------------------|-------------------------|-----------------------------------|----------------------|-----------------------------------|----------------------|-----------|
| Mode       | Symm.          | $\tilde{\nu}$ (cm <sup>-1</sup> ) | $\lambda$ ( $\mu$ m) | IR int. (km mol <sup>-1</sup> ) | Rel. int.               | $\tilde{\nu}$ (cm <sup>-1</sup> ) | $\lambda$ ( $\mu$ m) | $\tilde{\nu}$ (cm <sup>-1</sup> ) | $\lambda$ ( $\mu$ m) | Rel. int. |
| 1          | A <sub>1</sub> | 3042.9                            | 3.29                 | 2.22                            | 2                       | -                                 | -                    | -                                 | -                    | -         |
| 2          |                | 2920.6                            | 3.42                 | 21.43                           | 15                      | -                                 | -                    | -                                 | -                    | -         |
| 3          |                | 1446.4                            | 6.91                 | 0.15                            | 0                       | -                                 | -                    | 1423                              | 7.03                 | m         |
| 4          |                | 1356.7                            | 7.37                 | 2.46                            | 2                       | -                                 | -                    | 1359                              | 7.36                 | r         |
| 5          |                | 1247.9                            | 8.01                 | 139.27                          | 100                     | 1274 <sup>a</sup>                 | 7.85                 | 1269                              | 7.88                 | vs        |
| 6          |                | 985.0                             | 10.15                | 7.46                            | 5                       | -                                 | -                    | -                                 | -                    | -         |
| 7          |                | 685.8                             | 14.58                | 0.30                            | 0                       | -                                 | -                    | 704                               | 14.20                | r         |
| 8          |                | 363.5                             | 27.51                | 0.69                            | 0                       | 363 <sup>b</sup>                  | 27.548               | 380                               | 26.32                | s         |
| 9          | A <sub>2</sub> | 2953.0                            | 3.39                 | 0                               | -                       | -                                 | -                    | -                                 | -                    | -         |
| 10         |                | 1420.1                            | 7.04                 | 0                               | -                       | -                                 | -                    | 1447                              | 6.91                 | m         |
| 11         |                | 895.3                             | 11.17                | 0                               | -                       | -                                 | -                    | 992                               | 10.08                | m         |
| 12         |                | 79.1                              | 126.43               | 0                               | -                       | -                                 | -                    | -                                 | -                    | -         |
| 13         | B <sub>1</sub> | 2960.0                            | 3.38                 | 15.87                           | 11                      | -                                 | -                    | -                                 | -                    | -         |
| 14         |                | 1442.3                            | 6.93                 | 17.78                           | 13                      | -                                 | -                    | 1438                              | 6.95                 | r         |
| 15         |                | 1042.9                            | 9.59                 | 0.34                            | 0                       | -                                 | -                    | 1087                              | 9.20                 | vs        |
| 16         |                | 435.9                             | 22.94                | 2.04                            | 1                       | -                                 | -                    | 436                               | 22.94                | m         |
| 17         |                | 152.6                             | 65.53                | 0.50                            | 0                       | 153 <sup>b</sup>                  | 65.359               | -                                 | -                    | -         |
| 18         | B <sub>2</sub> | 3041.2                            | 3.29                 | 8.59                            | 6                       | -                                 | -                    | -                                 | -                    | -         |
| 19         |                | 2912.5                            | 3.43                 | 1.57                            | 1                       | -                                 | -                    | -                                 | -                    | -         |
| 20         |                | 1413.2                            | 7.08                 | 6.56                            | 5                       | -                                 | -                    | 1423                              | 7.03                 | m         |
| 21         |                | 1345.0                            | 7.44                 | 18.47                           | 13                      | -                                 | -                    | 1353                              | 7.39                 | m         |
| 22         |                | 1175.1                            | 8.51                 | 8.36                            | 6                       | -                                 | -                    | 1195                              | 8.37                 | m         |
| 23         |                | 902.2                             | 11.08                | 3.61                            | 3                       | -                                 | -                    | 896                               | 11.16                | r         |
| 23         | 374.7          | 26.68                             | 1.06                 | 1                               | -                       | -                                 | -                    | -                                 | -                    |           |

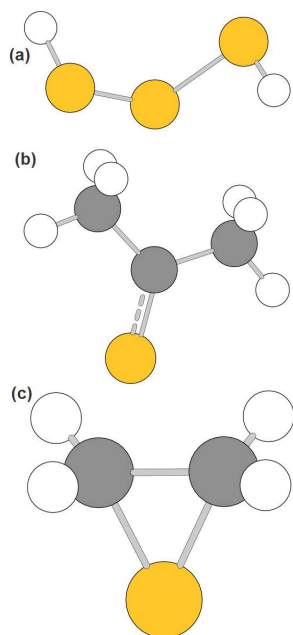
two bands with highest intensities (labeled bold in Table 8) belong to the interval around unidentified bands. Therefore, (CH<sub>2</sub>S)<sub>3</sub>, (CH<sub>2</sub>S)<sub>4</sub>, and C<sub>2</sub>H<sub>4</sub>S are good candidates for carriers of several unidentified bands observed by *ISO* (ISO 2002; Sturm et al. 2000; Lutz et al. 2000; Fischer et al. 1999). *ISO* observations showed that intensities of bands vary considerably depending on the extragalactic source (Sturm et al. 2000). The strongest calculated bands in Table 8 are at 3.3, 3.4, 8.3, 14.8, and 16.5  $\mu$ m. These positions agree with bands in some of objects observed by *ISO*. The band at 3.3 and its satellite at 3.4  $\mu$ m are strong in M82, NG253, 30 Doradus,

and Circinus. This feature is weaker in NGC 1068. The band at 8.3  $\mu$ m was observed only in M82, and it is not strong. The band at 14.8  $\mu$ m is also not strong. It was detected in M82, NGC253, 30 Doradus, and Circinus. The band at 16.5  $\mu$ m was observed in three galaxies. It is strong in M82 and NGC 253, whereas it is weak in the 30 Doradus region. Differences of intensities in observed spectra are results of different physical conditions in extragalactic objects.

Table 9 shows that in the proposed interval around unidentified bands are positioned five bands of S<sub>5</sub>CH<sub>2</sub>, nine of S<sub>6</sub>CH<sub>2</sub>, three of HSSSH, and ten of (CH<sub>3</sub>)<sub>2</sub>CS.

**Table 7.** Calculated (scaled by 0.9687) and measured <sup>a</sup>(Allen et al. 1986) vibrational fundamental bands for thiirane, C<sub>2</sub>H<sub>4</sub>S. Three IR inactive A<sub>2</sub> modes are omitted.

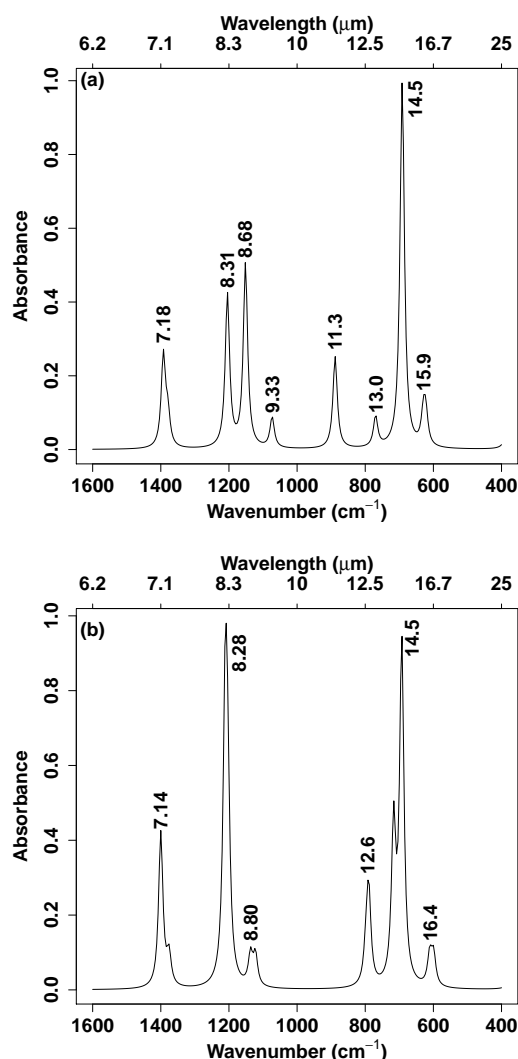
| Mode | Symm.          | Calculated                        |                      |                                 | Measured <sup>a</sup> |                                   |                      |
|------|----------------|-----------------------------------|----------------------|---------------------------------|-----------------------|-----------------------------------|----------------------|
|      |                | $\tilde{\nu}$ (cm <sup>-1</sup> ) | $\lambda$ ( $\mu$ m) | IR int. (km mol <sup>-1</sup> ) | Rel. int.             | $\tilde{\nu}$ (cm <sup>-1</sup> ) | $\lambda$ ( $\mu$ m) |
| 1    | A <sub>1</sub> | 3027.5                            | 3.30                 | 15.89                           | 62                    | 3014                              | 3.32                 |
| 2    |                | 1449.9                            | 6.90                 | 2.58                            | 10                    | 1457                              | 6.86                 |
| 3    |                | 1105.0                            | 9.05                 | 1.66                            | 6                     | 1109                              | 9.02                 |
| 4    |                | 1012.0                            | 9.88                 | 0.68                            | 3                     | 1024                              | 9.76                 |
| 5    |                | 599.6                             | 16.68                | 25.59                           | 100                   | 627                               | 15.95                |
| 9    | B <sub>1</sub> | 3115.5                            | 3.21                 | 3.36                            | 13                    | 3088                              | 3.24                 |
| 10   |                | 923.3                             | 10.83                | 3.24                            | 13                    | 945                               | 10.58                |
| 11   |                | 810.5                             | 12.34                | 0.57                            | 2                     | 824                               | 12.14                |
| 12   | B <sub>2</sub> | 3026.7                            | 3.30                 | 11.57                           | 45                    | 3013                              | 3.32                 |
| 13   |                | 1428.5                            | 7.00                 | 0.90                            | 4                     | 1436                              | 6.96                 |
| 14   |                | 1044.4                            | 9.57                 | 22.33                           | 87                    | 1051                              | 9.51                 |
| 15   |                | 637.6                             | 15.68                | 0.38                            | 1                     | -                                 | -                    |

**Figure 3.** The optimized structures: (a) *trans*-HSSSH, (b) (CH<sub>3</sub>)<sub>2</sub>CS (thioacetone), (c) C<sub>2</sub>H<sub>4</sub>S (thiirane). A double C-S bond in (CH<sub>3</sub>)<sub>2</sub>CS is shown. Details as in Fig. 1.

However, either two strongest bands (S<sub>5</sub>CH<sub>2</sub>, (CH<sub>3</sub>)<sub>2</sub>CS), or only the strongest one (S<sub>6</sub>CH<sub>2</sub>, HSSSH) do not belong to this interval. Because of high quality basis set that has been shown to produce accurate IR intensities (Zvereva, Shagidullin & Katsyuba 2011), S<sub>5</sub>CH<sub>2</sub>, S<sub>6</sub>CH<sub>2</sub>, HSSSH, and (CH<sub>3</sub>)<sub>2</sub>CS are less probable carriers of unidentified features observed in selected galactic sources by *ISO* (ISO 2002; Sturm et al. 2000; Lutz et al. 2000; Fischer et al. 1999).

### 3.2 Sulfur-bearing species in extragalactic molecular gases

Below we present the list of the presently detected (to the best of our knowledge) sulfur-bearing species in NGC

**Figure 4.** IR spectrum: (a) (CH<sub>2</sub>S)<sub>3</sub>, (b) (CH<sub>2</sub>S)<sub>4</sub>. Positions at the peaks are in  $\mu$ m.

**Table 8.** Comparison of unidentified lines and bands in the (2–200)  $\mu\text{m}$  range observed by *Infrared Space Observatory*<sup>a</sup> (ISO 2002; Sturm et al. 2000; Lutz et al. 2000; Fischer et al. 1999), and our results for the trimer and tetramer of thioformaldehyde, as well as for thiirane. The two strongest calculated bands are shown in bold and  $\Delta = 18.9 \text{ cm}^{-1}$  is the mean average error after using the scaling factor within the density functional theory calculation method.

| $\lambda$ ( $\mu\text{m}$ ) <sup>a</sup> | $\tilde{\nu}$ ( $\text{cm}^{-1}$ ) <sup>a</sup> | $\tilde{\nu}-\Delta$ ( $\text{cm}^{-1}$ ) | $\tilde{\nu}+\Delta$ ( $\text{cm}^{-1}$ ) | (CH <sub>2</sub> S) <sub>3</sub><br>$\tilde{\nu}$ ( $\text{cm}^{-1}$ ) | (CH <sub>2</sub> S) <sub>4</sub><br>$\tilde{\nu}$ ( $\text{cm}^{-1}$ ) | C <sub>2</sub> H <sub>4</sub> S<br>$\tilde{\nu}$ ( $\text{cm}^{-1}$ ) |
|--|---|---|---|--|--|---|
| 3.25                                     | 3076.92   | 3058.0                                    | 3095.8                                    | -  | -  | -   |
| -  | -   | -   | -   | -  | -  | 3115.5  |
| 3.3                                      | 3030.30   | 3011.4                                    | 3049.2                                    | 3028.7; 3027.2   | 3035.9; 3031.5   | <b>3027.5</b> ; 3026.7  |
| -  | -   | -   | -   | -  | 2980.7   | -   |
| -  | -   | -   | -   | -  | 2978.1   | -   |
| 3.4                                      | 2941.18   | 2922.3                                    | 2960.1                                    | 2953.4; <b>2947.9</b>  | -  | -   |
| 3.5                                      | 2857.14   | 2838.2                                    | 2876.0                                    | -  | -  | -   |
| 3.75                                     | 2666.67   | 2647.8                                    | 2685.6                                    | -  | -  | -   |
| 5.25                                     | 1904.76   | 1885.9                                    | 1923.7                                    | -  | -  | -   |
| 5.65                                     | 1769.91   | 1751.0                                    | 1788.8                                    | -  | -  | -   |
| 6.0                                      | 1666.67   | 1647.8                                    | 1685.6                                    | -  | -  | -   |
| 6.2                                      | 1612.90   | 1594.0                                    | 1631.8                                    | -  | -  | -   |
| 6.3                                      | 1587.30   | 1568.4                                    | 1606.2                                    | -  | -  | -   |
| -  | -   | -   | -   | -  | -  | 1449.9  |
| 7.0                                      | 1428.57   | 1409.7                                    | 1447.5                                    | -  | -  | 1428.5  |
| -  | -   | -   | -   | -  | 1400.1   | -   |
| -  | -   | -   | -   | 1392.5; 1379.4   | 1376.0   | -   |
| 7.555                                    | 1323.63   | 1304.7                                    | 1342.5                                    | -  | -  | -   |
| 7.6                                      | 1315.79   | 1296.9                                    | 1334.7                                    | -  | -  | -   |
| 7.8                                      | 1282.05   | 1263.2                                    | 1301.0                                    | -  | -  | -   |
| 8.3                                      | 1204.82   | 1185.9                                    | 1223.7                                    | 1204.5   | <b>1210.7</b> ; 1203.7   | -   |
| 8.6                                      | 1162.79   | 1153.9                                    | 1181.7                                    | -  | -  | -   |
| -  | -   | -   | -   | 1151.7   | -  | -   |
| -  | -   | -   | -   | -  | 1136.6   | -   |
| -  | -   | -   | -   | -  | 1122.2   | -   |
| -  | -   | -   | -   | -  | -  | 1105.0  |
| -  | -   | -   | -   | -  | -  | 1044.4  |
| -  | -   | -   | -   | -  | -  | 1012.0  |
| 10.6                                     | 943.40  | 924.5                                     | 962.3                                     | -  | -  | -   |
| -  | -   | -   | -   | -  | -  | 923.3   |
| 11.05                                    | 904.98  | 886.1                                     | 923.9                                     | -  | -  | -   |
| 11.25                                    | 888.89  | 870.0                                     | 907.8                                     | 888.4  | -  | -   |
| 12.0                                     | 833.33  | 814.4                                     | 852.2                                     | -  | -  | -   |
| -  | -   | -   | -   | -  | -  | 810.5   |
| 12.7                                     | 787.40  | 768.5                                     | 806.3                                     | 769.6  | 797.4; 789.7   | -   |
| 13.55                                    | 738.01  | 729.1                                     | 756.9                                     | -  | -  | -   |
| -  | -   | -   | -   | -  | 716.6  | -   |
| 14.25                                    | 701.75  | 682.8                                     | 720.6                                     | -  | -  | -   |
| 14.8                                     | 675.68  | 656.8                                     | 694.6                                     | <b>691.3</b>   | <b>692.8</b>   | -   |
| 15.7                                     | 636.94  | 618.0                                     | 655.8                                     | 629.2; 622.4   | -  | 637.6   |
| 16.5                                     | 606.06  | 587.2                                     | 625.0                                     | -  | 610.6; 599.4   | <b>599.6</b>  |
| 17.4                                     | 574.71  | 555.8                                     | 593.6                                     | -  | -  | -   |
| 18.0                                     | 555.56  | 536.7                                     | 574.5                                     | -  | -  | -   |
| -  | -   | -   | -   | 381.2  | -  | -   |
| -  | -   | -   | -   | -  | 365.3  | -   |
| 34.0                                     | 294.12  | 275.2                                     | 313.0                                     | -  | 278.5  | -   |
| -  | -   | -   | -   | 274.8  | -  | -   |
| -  | -   | -   | -   | 268.3  | -  | -   |
| -  | -   | -   | -   | -  | 195.2  | -   |
| 60.12                                    | 166.33  | 147.4                                     | 185.2                                     | -  | -  | -   |
| 74.24                                    | 134.70  | 119.5                                     | 153.6                                     | -  | 128.1  | -   |
| -  | -   | -   | -   | 169.4  | -  | -   |
| 77.155                                   | 129.61  | 110.7                                     | 148.5                                     | -  | -  | -   |
| 153.12                                   | 65.31   | 46.4                                      | 84.2                                      | -  | -  | -   |
| -  | -   | -   | -   | -  | 31.3   | -   |



**Table 9.** Comparison of unidentified lines and bands in the (2–200)  $\mu\text{m}$  range observed by *Infrared Space Observatory*<sup>a</sup>(ISO 2002; Sturm et al. 2000; Lutz et al. 2000; Fischer et al. 1999), and our results for pentathian, hexathiepan, trisulfane, and thioacetone. The two strongest calculated bands are shown in bold and  $\Delta = 18.9 \text{ cm}^{-1}$  is the mean average error after using the scaling factor within the density functional theory calculation method.

| $\lambda$ ( $\mu\text{m}$ ) <sup>a</sup> | $\tilde{\nu}$ ( $\text{cm}^{-1}$ ) <sup>a</sup> | $\tilde{\nu}-\Delta$ ( $\text{cm}^{-1}$ ) | $\tilde{\nu}+\Delta$ ( $\text{cm}^{-1}$ ) | S <sub>5</sub> CH <sub>2</sub>     |                                    | S <sub>6</sub> CH <sub>2</sub>     |                                    | HSSSH                              |                                    | (CH <sub>3</sub> ) <sub>2</sub> CS |   |
|--|---|---|---|------------------------------------|------------------------------------|------------------------------------|------------------------------------|------------------------------------|------------------------------------|------------------------------------|---|
|  |   |   |   | $\tilde{\nu}$ ( $\text{cm}^{-1}$ ) | $\tilde{\nu}$ ( $\text{cm}^{-1}$ ) | $\tilde{\nu}$ ( $\text{cm}^{-1}$ ) | $\tilde{\nu}$ ( $\text{cm}^{-1}$ ) | $\tilde{\nu}$ ( $\text{cm}^{-1}$ ) | $\tilde{\nu}$ ( $\text{cm}^{-1}$ ) |                                    |   |
| 3.25                                     | 3076.92   | 3058.0                                    | 3095.8                                    | -                                  | -                                  | -                                  | -                                  | -                                  | -                                  | -                                  | - |
| 3.3                                      | 3030.30   | 3011.4                                    | 3049.2                                    | 3024.4                             | -                                  | -                                  | -                                  | -                                  | -                                  | 3042.9; 3041.2                     | - |
| -  | -   | -   | -   | -                                  | 3006.8                             | -                                  | -                                  | -                                  | -                                  | -                                  | - |
| -  | -   | -   | -   | <b>2960.1</b>                      | -                                  | -                                  | -                                  | -                                  | -                                  | -                                  | - |
| 3.4                                      | 2941.18   | 2922.3                                    | 2960.1                                    | -                                  | 2951.7                             | -                                  | -                                  | -                                  | -                                  | 2960.0                             | - |
| -  | -   | -   | -   | -                                  | -                                  | -                                  | -                                  | -                                  | -                                  | <b>2920.6</b> ; 2912.5             | - |
| 3.5                                      | 2857.14   | 2838.2                                    | 2876.0                                    | -                                  | -                                  | -                                  | -                                  | -                                  | -                                  | -                                  | - |
| 3.75                                     | 2666.67   | 2647.8                                    | 2685.6                                    | -                                  | -                                  | -                                  | -                                  | -                                  | -                                  | -                                  | - |
| -  | -   | -   | -   | -                                  | -                                  | -                                  | 2548.6                             | -                                  | -                                  | -                                  | - |
| -  | -   | -   | -   | -                                  | -                                  | -                                  | 2547.1                             | -                                  | -                                  | -                                  | - |
| 5.25                                     | 1904.76   | 1885.9                                    | 1923.7                                    | -                                  | -                                  | -                                  | -                                  | -                                  | -                                  | -                                  | - |
| 5.65                                     | 1769.91   | 1751.0                                    | 1788.8                                    | -                                  | -                                  | -                                  | -                                  | -                                  | -                                  | -                                  | - |
| 6.0                                      | 1666.67   | 1647.8                                    | 1685.6                                    | -                                  | -                                  | -                                  | -                                  | -                                  | -                                  | -                                  | - |
| 6.2                                      | 1612.90   | 1594.0                                    | 1631.8                                    | -                                  | -                                  | -                                  | -                                  | -                                  | -                                  | -                                  | - |
| 6.3                                      | 1587.30   | 1568.4                                    | 1606.2                                    | -                                  | -                                  | -                                  | -                                  | -                                  | -                                  | -                                  | - |
| 7.0                                      | 1428.57   | 1409.7                                    | 1447.5                                    | -                                  | -                                  | -                                  | -                                  | -                                  | -                                  | 1446.4; 1442.3; 1413.2             | - |
| -  | -   | -   | -   | 1390.7                             | 1386.2                             | -                                  | -                                  | -                                  | -                                  | 1356.7; 1345.0                     | - |
| 7.555                                    | 1323.63   | 1304.7                                    | 1342.5                                    | -                                  | -                                  | -                                  | -                                  | -                                  | -                                  | -                                  | - |
| 7.6                                      | 1315.79   | 1296.9                                    | 1334.7                                    | -                                  | -                                  | -                                  | -                                  | -                                  | -                                  | -                                  | - |
| 7.8                                      | 1282.05   | 1263.2                                    | 1301.0                                    | -                                  | -                                  | -                                  | -                                  | -                                  | -                                  | -                                  | - |
| -  | -   | -   | -   | -                                  | -                                  | -                                  | -                                  | -                                  | -                                  | <b>1247.9</b>                      | - |
| 8.3                                      | 1204.82   | 1185.9                                    | 1223.7                                    | -                                  | -                                  | -                                  | -                                  | -                                  | -                                  | -                                  | - |
| 8.6                                      | 1162.79   | 1153.9                                    | 1181.7                                    | 1175.6                             | <b>1175.2</b>                      | -                                  | -                                  | -                                  | -                                  | 1175.1                             | - |
| -  | -   | -   | -   | 1084.8                             | 1094.9                             | -                                  | -                                  | -                                  | -                                  | 1042.9; 985.0                      | - |
| 10.6                                     | 943.40  | 924.5                                     | 962.3                                     | -                                  | -                                  | -                                  | -                                  | -                                  | -                                  | -                                  | - |
| 11.05                                    | 904.98  | 886.1                                     | 923.9                                     | -                                  | -                                  | -                                  | -                                  | -                                  | -                                  | 902.2                              | - |
| 11.25                                    | 888.89  | 870.0                                     | 907.8                                     | -                                  | -                                  | -                                  | -                                  | -                                  | -                                  | -                                  | - |
| 12.0                                     | 833.33  | 814.4                                     | 852.2                                     | -                                  | -                                  | -                                  | 841.9; 829.2                       | -                                  | -                                  | -                                  | - |
| -  | -   | -   | -   | 813.0                              | -                                  | -                                  | -                                  | -                                  | -                                  | -                                  | - |
| 12.7                                     | 787.40  | 768.5                                     | 806.3                                     | -                                  | 790.8                              | -                                  | -                                  | -                                  | -                                  | -                                  | - |
| 13.55                                    | 738.01  | 729.1                                     | 756.9                                     | -                                  | -                                  | -                                  | -                                  | -                                  | -                                  | -                                  | - |
| 14.25                                    | 701.75  | 682.9                                     | 720.6                                     | -                                  | 688.0                              | -                                  | -                                  | -                                  | -                                  | 685.8                              | - |
| 14.8                                     | 675.68  | 656.8                                     | 694.6                                     | 670.2                              | -                                  | -                                  | -                                  | -                                  | -                                  | -                                  | - |
| 15.7                                     | 636.94  | 618.0                                     | 655.8                                     | -                                  | -                                  | -                                  | -                                  | -                                  | -                                  | -                                  | - |
| 16.5                                     | 606.06  | 587.2                                     | 625.0                                     | 599.4                              | 591.3                              | -                                  | -                                  | -                                  | -                                  | -                                  | - |
| 17.4                                     | 574.71  | 555.8                                     | 593.6                                     | -                                  | -                                  | -                                  | -                                  | -                                  | -                                  | -                                  | - |
| 18.0                                     | 555.56  | 536.7                                     | 574.5                                     | -                                  | -                                  | -                                  | -                                  | -                                  | -                                  | -                                  | - |
| -  | -   | -   | -   | 486.0                              | 460.5                              | -                                  | 458.8                              | -                                  | -                                  | -                                  | - |
| -  | -   | -   | -   | 474.4                              | 456.6                              | -                                  | <b>438.2</b>                       | -                                  | -                                  | -                                  | - |
| -  | -   | -   | -   | <b>417.9</b>                       | <b>448.3</b>                       | -                                  | -                                  | -                                  | -                                  | -                                  | - |
| -  | -   | -   | -   | 357.6                              | 403.0                              | -                                  | -                                  | -                                  | -                                  | -                                  | - |
| -  | -   | -   | -   | 342.5                              | 373.0                              | -                                  | -                                  | -                                  | -                                  | 435.9                              | - |
| -  | -   | -   | -   | -                                  | 347.3                              | -                                  | 322.2                              | -                                  | -                                  | 374.7; 363.5                       | - |
| 34.0                                     | 294.12  | 275.2                                     | 313.0                                     | -                                  | -                                  | -                                  | <b>303.4</b>                       | -                                  | -                                  | -                                  | - |
| -  | -   | -   | -   | 241.5                              | 270.6                              | -                                  | -                                  | -                                  | -                                  | -                                  | - |
| -  | -   | -   | -   | 222.0                              | 228.7                              | -                                  | -                                  | -                                  | -                                  | -                                  | - |
| -  | -   | -   | -   | 189.9                              | 193.0                              | -                                  | 193.7                              | -                                  | -                                  | -                                  | - |
| 60.12                                    | 166.33  | 147.4                                     | 185.2                                     | 173.2                              | 174.8; 161.3                       | -                                  | -                                  | -                                  | -                                  | 152.6                              | - |
| 74.24                                    | 134.70  | 119.5                                     | 153.6                                     | -                                  | -                                  | -                                  | -                                  | -                                  | -                                  | -                                  | - |
| 77.155                                   | 129.61  | 110.7                                     | 148.5                                     | -                                  | 111.0                              | -                                  | -                                  | -                                  | -                                  | -                                  | - |
| 153.12                                   | 65.31   | 46.4                                      | 84.2                                      | -                                  | -                                  | -                                  | -                                  | -                                  | -                                  | -                                  | - |
| -  | -   | -   | -   | 35.2                               | -                                  | -                                  | -                                  | -                                  | -                                  | -                                  | - |

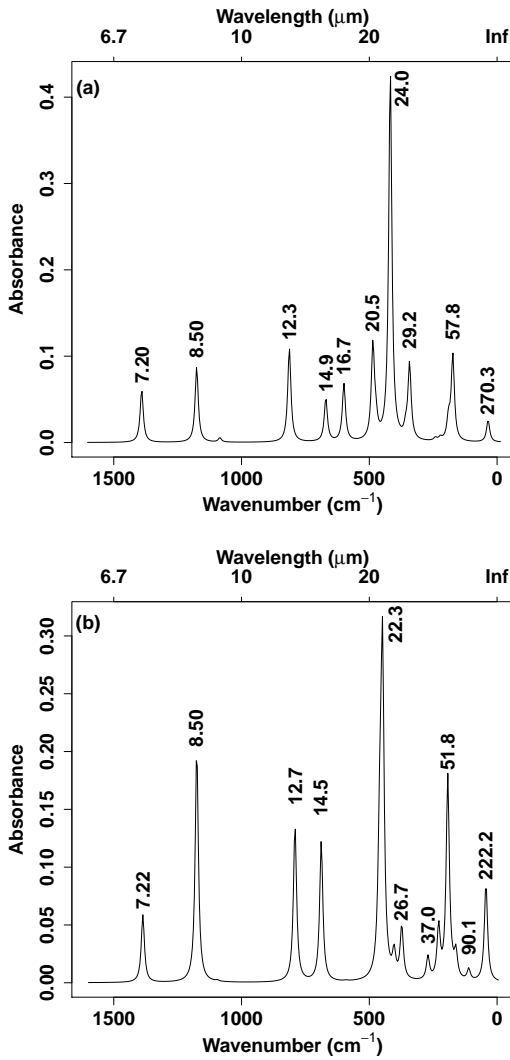


**Figure 5.** IR spectrum of: (a) S<sub>5</sub>CH<sub>2</sub>, (b) S<sub>6</sub>CH<sub>2</sub>. Positions at the peaks are in μm.

253, M82, NGC1068, Circinus, Arp 220, and 30 Doradus. These objects were observed by *ISO* and unidentified features were found (ISO 2002; Sturm et al. 2000; Lutz et al. 2000; Fischer et al. 1999). Ultraviolet, X-ray, and cosmic-ray irradiations, as well as shocks, are present in these galaxies and determine the chemical processes in molecular gases for sulfur-bearing and other species. For example, it was found in laboratories on Earth that UV and X-ray irradiations catalyze the formation of (CH<sub>2</sub>S)<sub>3</sub> and (CH<sub>2</sub>S)<sub>4</sub> from H<sub>2</sub>CO and H<sub>2</sub>S (Credali & Russo 1967). Therefore, favorable conditions for the formation of (CH<sub>2</sub>S)<sub>n</sub> exist in extragalactic molecular gases.

NGC 253 is also known as the Sculptor, or the Silver dollar galaxy. It is the bright, spiral, starburst galaxy where many molecular lines have been detected. Sulfur-bearing species H<sub>2</sub>S, CS, C<sub>2</sub>S, NS, SO, H<sub>2</sub>CS, OCS, and SO<sub>2</sub> were observed in the nuclear region of NGC 253 using the *IRAM* 30 m and the Swedish-ESO Submillimetre Telescope (*SEST*) (Martin et al. 2005, 2006). It was proposed that turbulent motions and shocks release H<sub>2</sub>S and OCS from grain mantles into the gas phase. Then other sulfur-bearing species

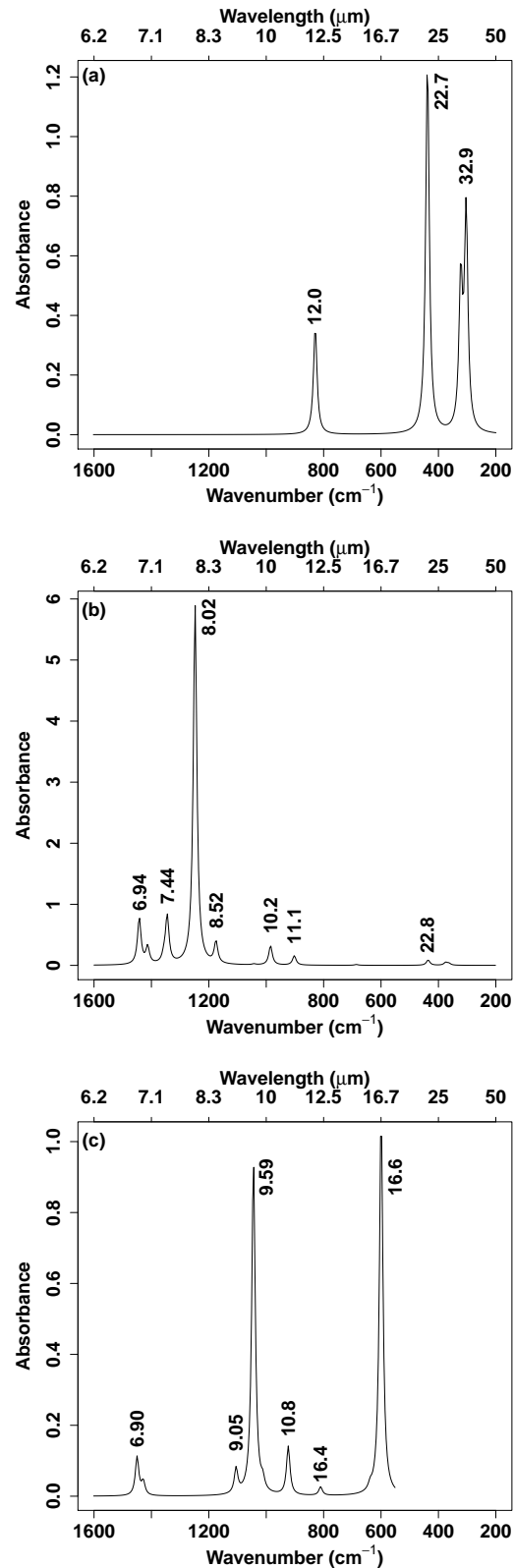


**Figure 6.** IR spectrum of: (a) *trans*-HSSSH, (b) (CH<sub>3</sub>)<sub>2</sub>CS, (c) C<sub>2</sub>H<sub>4</sub>S. Positions at the peaks are in μm.

are formed in the gas-phase chemistry processes. Relative abundances of sulfur-bearing molecules in different environments suggest that the chemical processes in the nuclear region of NGC 253 are similar to those in the Sgr B2 envelope in the galactic center (Martin et al. 2008). Low-velocity large scale shocks were found responsible for the similar sulfur chemistry in these two regions. Both formaldehyde (Gardner & Whiteoak 1974) and  $\text{H}_2\text{S}$  (Martin et al. 2005, 2006), which react in laboratories under irradiation and form  $(\text{CH}_2\text{S})_n$ , were detected in NGC 253.

M82, also known as NGC 3034 or Cigar, is an irregular starburst galaxy. It was found that the chemical processes in M82 and NGC 253 are different (Martin et al. 2006; Aladro et al. 2011). Although both galaxies are starburst, they are at the different evolutionary stage. M82 is more evolved starburst where photodissociation regions (Tielens & Hollenbach 1985) are dominant in the heating of the molecular gas. These processes are driven by ultraviolet photons from young stars. Molecular abundances in M82 are similar to the well studied photon-dominated region the Orion bar. Photon-dominated regions are also present in NGC 253 (Martin, Martin-Pintado & Viti 2009), but they do not drive the heating of molecular clouds. *IRAM* 30 m telescope was used to study the chemical species in the central parts of M82 (Aladro et al. 2011). Among eighteen detected molecules several sulfur species were found:  $\text{H}_2\text{S}$ ,  $\text{H}_2\text{CS}$ , CS, SO, and  $\text{SO}_2$ . Formaldehyde was also detected in M82 (Aladro et al. 2011) and could under irradiation react with  $\text{H}_2\text{S}$  to form  $(\text{CH}_2\text{S})_n$ .

NGC 1068, also known as M77, is a barred, spiral, active galaxy. Although NGC 1068 is with an active galactic nucleus, it also contains the starburst ring (Takano et al. 2014; García-Burillo et al. 2014; Viti et al. 2014). The chemical composition of molecular clouds in NGC 1068 was studied by the *IRAM* 30 m telescope (Aladro et al. 2013). Seventeen molecules and seven isotopologues were detected and among them sulfur species SO, NS, and CS. The results for NGC 1068 were compared to the starburst galaxies M82 and NGC 253. Some sulfur molecules which were detected in two starburst galaxies, such as OCS,  $\text{SO}_2$ ,  $\text{C}_2\text{S}$ ,  $\text{H}_2\text{S}$ , and  $\text{H}_2\text{CS}$ , have not been yet found in NGC 1068. Recently NGC 1068 was studied using the Atacama Large Millimeter Array (*ALMA*) (Takano et al. 2014; García-Burillo et al. 2014; Viti et al. 2014). Takano and coworkers studied several molecular transitions (including those in sulfur species CS and SO) in the central region of NGC 1068. García-Burillo and coworkers (García-Burillo et al. 2014), as well as Viti and coworkers (Viti et al. 2014) also investigated the molecular gas in NGC 1068 using the *ALMA* telescope. They mapped the emission of several tracers (including CS) and underlying continuum emission of the circumnuclear disk and the starburst ring.

The Circinus galaxy is an active, starburst, spiral galaxy. NGC 1068 and Circinus are similar. Both are typical Seyfert 2 galaxies close to the Milky Way and contain the molecular gas which surrounds nuclei, as well as star-forming rings (Zhang et al. 2014). Several molecular transitions, and among them in sulfur species CS and SO, were observed in the study of a dense molecular gas in the central part of the Circinus galaxy using the *SEST* telescope (Curran et al. 2001).

Arp 220 is an ultra-luminous infrared galaxy (ULIRG)

closest to Earth. This elliptical galaxy is the merger system and contains a star-forming region as well as a double nucleus. The prebiotic molecule methanimine ( $\text{CH}_2\text{NH}$ ) was detected in Arp 220 (Salter et al. 2008). The molecular composition of Arp 220 was studied using the Submillimeter Array (*SMA*) in Mauna Kea, Hawaii (Martín et al. 2011). Fifteen molecular species and six isotopologues were observed, and among them sulfur-bearing molecules:  $\text{H}_2\text{S}$ , SO, NS, and CS. Formaldehyde was also detected.

The star-forming region 30 Doradus in the Large Magellanic cloud, also known as the Tarantula nebula or NGC 2070, is the most active in the Local group. Heikkilä and coworkers studied molecular abundances in 30 Doradus using the *SEST* telescope (Heikkilä, Johansson & Olofsson 1999). They detected several molecular transitions and among them in CS and SO. The sulfur-bearing molecule CS in 30 Doradus was also observed by Rubio and coworkers using *SEST* (Rubio, Paron & Dubner 2009), and in recent studies by the *ALMA* telescope (Indebetouw et al. 2013).

We find that all six bright bands from Table 8 agree with features observed in M82. Five strong calculated bands agree with observed features in NGC 253 and 30 Doradus, three in Circinus, and only one in NGC 1068. Therefore, starburst galaxies are more favorable for the formation of  $(\text{CH}_2\text{S})_3$ ,  $(\text{CH}_2\text{S})_4$ , and  $\text{C}_2\text{H}_4\text{S}$ . This is especially true for M82, an evolved starburst with main processes driven by UV photons, where all six calculated bright bands were observed.

### 3.3 Sulfur-bearing species in galactic molecular gases: Orion KL and Sgr B2

Orion KL and Sgr B2 are well known galactic molecular clouds where star-forming is pronounced (Goicoechea 2008). They both were investigated by *ISO* in the far-IR region where they are in the group of the brightest sources.

Orion KL was investigated in the (486-492) GHz and (541-577) GHz intervals by the *Odin* satellite, and 280 spectral lines were observed from 38 molecules (Persson et al. 2007). Among them 64 lines were unidentified. Several sulfur species were detected:  $\text{SO}_2$ , SO,  $\text{H}_2\text{CS}$ ,  $\text{H}_2\text{S}$ , OCS, CS,  $\text{HCS}^+$ , as well as formaldehyde. Tentative assignments were done for SiS,  $\text{SH}^-$ , and  $\text{SO}^+$ . Sulfur-bearing species in Orion KL were also studied with the *IRAM* 30 m telescope in the (80-115.5) GHz, (130-178) GHz, and (197-281) GHz intervals (Tercero et al. 2010; Esplugues et al. 2013). More than 14400 spectral features were detected and 10040 were identified and attributed to 43 molecules, among them to sulfur species: OCS,  $\text{HCS}^+$ ,  $\text{H}_2\text{CS}$ , CS, CCS,  $\text{C}_3\text{S}$ , SO, and  $\text{SO}_2$ . These results (Persson et al. 2007; Tercero et al. 2010; Esplugues et al. 2013) show that rich sulfur chemistry takes place in Orion KL. We find that two bands calculated for  $\text{S}_5\text{CH}_2$  (52.65 and 57.72  $\mu\text{m}$  in our Table 3) are close to unidentified bands at 52.57 and 58.02  $\mu\text{m}$  observed by *ISO* in the Orion KL (see their Table 10) (Lerate et al. 2006). However, Lerate and coworkers observed only the far-IR region (44-188)  $\mu\text{m}$ , whereas the majority of the bands we calculate for pentathian (as well as for other sulfur molecules studied in this work) are in the near and mid-IR.

It was proposed that similar sulfur chemistry exists in the nucleus of the starburst galaxy NGC 253 and Sgr B2 in the galactic center (Martin et al.

2008). Sgr B2 was studied with *ISO* in the near/mid-IR (Lutz et al. 1996) and in the far-IR region (Goicoechea, Rodriguez-Fernandez & Cernicharo 2004; Polehampton et al. 2007), but the attention was not devoted to the sulfur-bearing species. However, some unidentified features were observed (Polehampton et al. 2007). The *Mopra* 3-mm spectral line survey confirms that several sulfur-bearing molecules exist in Sgr B2 (Armijos-Abendaño et al. 2014). These are: CCS, OCS, CS, SiS, HCS<sup>+</sup>, SO<sub>2</sub>, and HNCS. Several unidentified lines were also observed. Sulfur-bearing species H<sub>2</sub>S, SO, SO<sub>2</sub>, H<sub>2</sub>CS, OCS, NS, SH<sup>+</sup>, and HCS<sup>+</sup> were observed in Sgr B2 by the *Herschel* telescope molecular line survey in the (157–625) μm range (Neill et al. 2014).

#### 4 CONCLUSIONS

Astrochemistry of sulfur is still unknown. We calculated IR spectra of several sulfur-bearing molecules and proposed that they take the role in the balance of the sulfur in dense clouds and comets. We studied ring molecules (CH<sub>2</sub>S)<sub>3</sub>, (CH<sub>2</sub>S)<sub>4</sub>, pentathian (S<sub>5</sub>CH<sub>2</sub>), hexathiepan (S<sub>6</sub>CH<sub>2</sub>), thiirane (C<sub>2</sub>H<sub>4</sub>S), and in addition two other sulfur-bearing molecules trisulfane (HSSSH) and thioacetone ((CH<sub>3</sub>)<sub>2</sub>CS). We found that calculated bands of (CH<sub>2</sub>S)<sub>3</sub>, (CH<sub>2</sub>S)<sub>4</sub>, and C<sub>2</sub>H<sub>4</sub>S agree with several unidentified features observed by *ISO* in starburst galaxies (M82, NGC 253, the 30 Doradus star-forming region in the Large Magellanic Cloud), and galaxies with active galactic nuclei (NGC 1068, Circinus). Studies of molecular compositions of several of these extragalactic objects on *ALMA* are still in progress. Many star-forming and other objects exist, and could act as the place with rich sulfur chemistry. Galactic objects where complex sulfur-bearing species could easily form are Orion KL and Sgr B2. We hope that a high resolution and sensitivity of *ALMA*, and in the future of the *James Webb Space Telescope* in the infrared spectral region, will enable detection of larger sulfur-bearing molecules.

#### ACKNOWLEDGMENTS

This work was done using the CRO-NGI e-grid and the computational cluster “Isabella” at the University of Zagreb Computing Centre SRCE. G. Bilalbegović acknowledges the support of the University of Zagreb research fund, grant “Physics of Stars and Cosmic Dust”. We are grateful to Guillermo Manuel Muñoz Caro for the useful correspondence, as well as for sending his PhD thesis and the article (Jiménez-Escobar, Muñoz Caro & Chen 2014) prior publication. This research has made use of NASA’s Astrophysics Data System Bibliographic Services. We thank the referee for constructive comments.

#### REFERENCES

Aladro R., Martín S., Martín-Pintado J., Mauersberger R., Henkel C., Ocana Flaquer B., Amo-Baladron M. A., 2011, *A&A*, 535, A84  
Aladro R. et al., 2013, *A&A*, 549, A39

Allen W. D., Bertie J. E., Falk M. V., Hess Jr. B. A., Mast G. B., Othen D. A., Schaad L. J., Schaefer III H. F., 1986, *J. Chem. Phys.*, 84, 4211  
Anderson D. E., Bergin E. A., Maret S., Wakelam V., 2013, *ApJ*, 779, 141  
Antolinez S., Lesarri A., Mata S., Blanco S., Lopez J. C., Alonso J. L., 2002, *J. Mol. Struct.*, 612, 125  
Armijos-Abendaño J., Martín-Pintado J., Requena-Torres M. A., Martín S., Rodríguez-Franco A., 2014, *ArXiv e-prints*: 1410.5762  
Bane M. K., Thompson C. D., Appadoo D. R. T., McNaughton D., 2012, *J. Chem. Phys.*, 137, 084306  
Barone V., Bloino J., Guido C. A., Lippardini F., 2010, *Chem. Phys. Lett.*, 496, 157  
Bauschlicher C. W. et al., 2010, *ApJS*, 189, 341  
Becke A. D., 1993, *J. Chem. Phys.*, 98, 5648  
Becke A. D., 2014, *J. Chem. Phys.*, 301, 5648  
Bell M. B., Feldman P. A., Travers M. J., McCarthy M. C., Gottlieb C. A., Thaddeus P., 1997, *ApJ*, 483, L61  
Biver N. et al., 1997, *Science*, 275, 1915  
Bloino J., Barone V., 2012, *J. Chem. Phys.*, 136, 124108  
Bockelée-Morvan D. et al., 2000, *A&A*, 353, 1101  
Boersma C. et al., 2014, *ApJS*, 211, 8  
Buckle J. V., Fuller G. A., 2003, *A&A*, 399, 567  
Cervellati R., Corbelli G., Lister D. G., 1984, *J. Mol. Struct.*, 117, 247  
Charnley S. B., 1997, *ApJ*, 481, 396  
Credali L., Russo M., 1967, *Polymer*, 8, 469  
Crovisier J., Leech K., Bockelée-Morvan D., Brooke T. Y., Hanner M. S., Altieri B., Uwe Keller H., Lellouch E., 1997, *Science*, 275, 1904  
Curran S. J., Johansson L. E. B., Bergman P., Heikkilä A., Aalto S., 2001, *A&A*, 568, A122  
Dickens J. E., Irvine W. M., Ohishi M., Ikeda M., Ishikawa S., Nummelin A., Hjalmarsen A., 1997, *ApJ*, 489, 753  
Dorofeeva O. V., Gurvich L. V., 1995, *J. Phys. Chem. Ref. Data*, 24, 1351  
Druard C., Wakelam V., 2012, *MNRAS*, 426, 354  
Ellestad O. H., Klaboe P., Hagen G., Stroyer-Hansen T., 1972, *Spectrochim. Acta A*, 28, 149  
Esplugues G. B., Tercero B., Cernicharo J., Goicoechea J. R., Palau A., Marcelino N., Bell T. A., 2013, *A&A*, 556, A143  
Ferrante R. F., Moore M. H., Spiliotis M. M., Hudson R. L., 2008, *ApJ*, 684, 1210  
Festou M., Uwe Keller H., Weaver H. A., eds., 2004, *Comets II*, University of Arizona Press, p. 391  
Fischer J. et al., 1999, *Ap&SS*, 266, 91  
Frisch M. J. et al., 2013, *Gaussian 09 Revision D.01*. Gaussian Inc. Wallingford CT 2009  
García-Burillo S. et al., 2014, *A&A*, arXiv:1405.7706  
Gardner F. F., Whiteoak J. B., 1974, *Nature*, 247, 526  
Garozzo M., Fulvio D., Kanuchova Z., Palumbo M. E., Strazzulla G., 2010, *A&A*, 509, A67  
Garrigou-Lagrange and C. G. Andrieu and Y. Mollier C., 1974, *Spectrochim. Acta A*, 32, 477  
Gibb E., Nummelin A., Irvine W. M., Whittet D. C. B., Bergman P., 2000, *ApJ*, 545, 309  
Goicoechea J. R., 2008, *EAS Publications Series*, 31, 73  
Goicoechea J. R., Rodriguez-Fernandez N. J., Cernicharo J., 2004, *ApJ*, 600, 214  
Goumans T. P. M., Bromley S. T., 2011, *MNRAS*, 414,

- 1285
- Heikkilä A., Johansson L. E. B., Olofsson H., 1999, *A&A*, 344, 817
- Hirao T., Okabayashi T., Tanimoto M., 2001, *J. Mol. Spectrosc.*, 208, 148
- Hirose C., Okiye K., Maeda S., 1976, *B. Chem. Soc. Jpn.*, 49, 916
- Indebetouw R. et al., 2013, *ApJ*, 774, 73
- ISO, 2002, Unidentified lines and bands in the 2-200  $\mu\text{m}$  range. 'http://www.ipac.caltech.edu/iso/lws/unidentified.html'
- Jacox M. E., 1994, *J. Phys. Chem. Ref. Data*, Monograph 3, updated data in NIST Chemistry Webbook: <http://webbook.nist.gov/chemistry/>
- Jiménez-Escobar A., Muñoz Caro G. M., 2011, *A&A*, 536, A91
- Jiménez-Escobar A., Muñoz Caro G. M., Chen Y. J., 2014, *MNRAS*, 443, 343
- Jiménez-Escobar A., Muñoz Caro G. M., Ciaravella A., Cecchi-Pastellini C., Candia R., Micela G., 2012, *ApJ*, 751, L40
- Keller L. P. et al., 2002, *Nature*, 417, 148
- Kirchner B., Huber H., Steinebrunner G., Dreizler H., Grabow J. U., Merke I., 1997, *Z. Naturforsch.*, 52, 297
- Klaboe P., 1969, *Spectrochim. Acta A*, 25, 1437
- Kolesnikova L., Tercero B., Cernicharo J., Alonso J. L., Daly A. M., 2014, *ApJ*, 784, L7
- Kroto H. W., Landsberg B. M., Suffolk R. J., Vodden A., 1974, *Chem. Phys. Lett.*, 29, 265
- Lerate M. R. et al., 2006, *MNRAS*, 370, 597
- Liedtke M. et al., 1993, *J. Phys. Chem.*, 97, 11204
- Liedtke M., Yamada K. M. T., Winnewisser G., Hahn J., 1997, *J. Mol. Struct.*, 413, 265
- Linke R. A., Frerking M. A., Thaddeus P., 1979, *ApJ*, 234, L139
- Lipscomb R. D., Sharkey W. H., 1970, *J. Polymer Sci. A*, 18, 2187
- Lutz D. et al., 1996, *A&A*, 315, L269
- Lutz D., Sturm E., Genzel R., Moorwood A. F. M., Alexander T., Netzer H., Sternberg A., 2000, *ApJ*, 536, 697
- Maeda A. et al., 2008, *ApJS*, 176, 543
- Martín S. et al., 2011, *A&A*, 527, A36
- Martin S., Martin-Pintado J., Mauersberger R., Henkel C., Garcia-Burillo S., 2005, *ApJ*, 620, 210
- Martin S., Martin-Pintado J., Viti S., 2009, *ApJ*, 706, 1323
- Martin S., Mauersberger R., Martin-Pintado J., Henkel C., Garcia-Burillo S., 2006, *ApJS*, 164, 450
- Martin S., Requena-Torres M. A., Martin-Pintado J., Mauersberger R., 2008, *ApJ*, 678, 245
- Muñoz Caro G. M., 2002, PhD thesis, Leiden University
- Nash C. P., Kenneth Musker W., Lam A. P. J., 1988, *Appl. Spectrosc.*, 42, 494
- Neill J. L. et al., 2014, *ApJ*, 789, 8
- NIST, 2014, Chemistry webbook. 'http://webbook.nist.gov/chemistry'
- Palumbo M. E., Geballe T. R., Tielens A. G. G. M., 1997, *ApJ*, 479, 839
- Peach M. E., Weissflog E., Pelz N., 1975, *J. Mass. Spectrom.*, 10, 781
- Penzias A. A., Solomon P. M., Wilson R. W., Jefferts K. B., 1971, *ApJ*, 168, L53
- Person W. B., Zerbi G., 1982, *Vibrational Intensities in Infrared and Raman Spectroscopy*. Elsevier, Amsterdam
- Persson C. M. et al., 2007, *A&A*, 476, 807
- Polehampton E. T., Baluteau J.-P., Swinyard B. M., Goicoechea J. R., Brown J. M., White G. J., Cernicharo J., Grundy T. W., 2007, *MNRAS*, 377, 1122
- Puzzarini C., Biczysko M., Bloino J., Barone V., 2014, *ApJ*, 785, 1
- Ricca A., Bauschlicher C. W., Boersma C., Tielens A. G. G. M., Allamandola L. J., 2012, *ApJ*, 754, 75
- Rubio M., Paron S., Dubner G., 2009, *A&A*, 505, 177
- Ruffle D. P., Hartquist T. W., Caselli P., Williams D. A., 1999, *MNRAS*, 306, 691
- Salter C. J., Ghosh T., Catinella B., Lebron M., Lerner M. S., Minchin R., Momjian E., 2008, *AJ*, 136, 389
- Scappini F., Cecchi-Pestellini C., Smith H., Klemperer W., Dalgarno A., 2003, *MNRAS*, 341, 657
- Shimanouchi T., 1972, *Tables of Molecular Vibrational Frequencies, Consolidated Volume 1*. National Standard Reference Data System, Washington, D.C.
- Sinclair M. W., Fourikis N., Ribes J. C., Robinson B. J., Brown R., Godfrey P. D., 1973, *Aust. J. Phys.*, 26, 85
- Snyder L. E., Buhl D., Zuckerman B., Palmer P., 1969, *Phys. Rev. Lett.*, 22, 679
- Stephens P. J., Devlin F. J., Chabrowski C. F., Frish M. J., 1994, *J. Chem. Phys.*, 98, 11623
- Sturm E., Lutz D., Tran D., Feuchtgruber H., Genzel R., Kunze D., Moorwood A. F. M., Thornley M. D., 2000, *A&A*, 358, 481
- Sverdlov L. M., Kovner M. A., Krainov E. P., 1974, *Vibrational Spectra of Polyatomic Molecules*. Wiley, New York
- Takano S. et al., 2014, *PASJ*, 66, 75
- Tercero B., Cernicharo J., Pardo J. R., Goicoechea J. R., 2010, *AA*, 517, A96
- Thaddeus P., Kutner M. L., Penzias A. A., Wilson R. W., Jefferts K. B., 1972, *ApJ*, 176, L73
- Tieftrunk A., des Forets G. P., Schilke P., Walmsley C. M., 1994, *A&A*, 289, 579
- Tielens A. G. G. M., 2013, *Rev. Mod. Phys.*, 85, 1021
- Tielens A. G. G. M., Hollenbach D., 1985, *ApJ*, 291, 722
- Tielens A. G. G. M., Whittet D. C. B., 1997, in *Molecules in Astrophysics*, van Dishoeck E. F., ed., Dordrecht: Kluwer, p. 45
- Viti S. et al., 2014, *A&A*, arXiv:1407.4940
- Watanabe N., Kouchi A., 2002, *ApJ*, 571, L173
- Wiesner H., Krueger P. J., Muller E., Hyne J. B., 1969, *Can. J. Chem.*, 47, 1633
- Woodney L. M., A'Hearn M. F., McMullin J., Samarasingha N., 1997, *Earth Moon Planets*, 78, 69
- Woon D. E., Dunning T. H., 1993, *J. Chem. Phys.*, 98, 1358
- Zasowski G., Kemper F., Watson D. M., Furlan E., Bohac C. J., Hull C., Green J. D., 2009, *ApJ*, 694, 459
- Zhang Z.-Y. et al., 2014, *A&A*, 367, 457
- Zvereva E. E., Shagidullin A. R., Katsyuba S. A., 2011, *J. Phys. Chem. A*, 115, 63